BEAM TEST RESULTS OF UNDULATOR CAVITY BPM ELECTRONICS FOR THE EUROPEAN XFEL

M. Stadler*, R. Baldinger, R. Ditter, B. Keil, R. Kramert, G. Marinkovic, M. Roggli, PSI, Villigen, Switzerland
D. Lipka, D. Nölle, M. Pelzer, S. Vilcins-Czvitkovits, DESY, Hamburg, Germany

Abstract

The European X-ray Free Electron Laser (E-XFEL) will use dual-resonator cavity BPMs (CBPMs) between the SASE undulators and in the beam transfer lines to measure and stabilize the beam trajectory. The BPM electronics is developed by PSI, while the pickup mechanics is developed by DESY. BPM electronics beam tests with three adjacent pickups have been performed at the SwissFEL injector test facility (SITF) at PSI. The system architecture and algorithms, achieved performance and noise correlation measurements of the present electronics prototypes will be presented.

INTRODUCTION

The European XFEL (E-XFEL) [1] has a superconducting 17.5GeV main linac that will provide trains of up to 2700 bunches, with 0.1-1nC bunch charge range, 600µs train length, ≥222ns bunch spacing, and 10Hz train repetition rate. A kicker/septum scheme can distribute fractions of the bunch train to two main SASE undulator lines followed by "secondary undulators" for spontaneous or FEL radiation. The E-XFEL will provide SASE radiation down to below 0.1nm wavelength and supports arbitrary bunch patterns within a bunch train, with bunch spacing of n*111ns, where n is an integer >1.

The E-XFEL is presently under construction in Hamburg, with first injector beam scheduled for 2014 and first main linac beam and SASE for 2015.

The cavity BPM electronic system is being developed at PSI [2,3]. For preliminary performance measurements an array of 3 E-XFEL cavity BPMs have been installed at the SwissFEL injector test facility [4].

CAVITY PICKUP

The 3.3 GHz cavity pickups were designed at DESY [5]. They have the parameters given in Table 1.

Table 1: Undulator cavity BPM pickup parameters (10mm beam pipe aperture)

	position cavity (TM110 mode)	reference cavity (TM010 mode)
Resonant frequency	3300 MHz	3300 MHz
Sensitivity	2.8 mV/nC/µm	42 V/nC
Cavity loaded-Q	70	70

*markus.stadler@psi.ch

BPM ELECTRONICS

The present BPM electronics prototype consists of:

- The RF front-end electronics (RFFE): One I/Q downconverter and LO synthesizer for reference, x- and y-position signal channel, and an ADC sampling clock synthesizer. Active local temperature stabilizers are employed for drift reduction.
- 6-channel, 16-bit 160MS/s analog-to-digital converters for all RFFE I and Q baseband differential output signals.
- Digital signal processing hardware ("GPAC" board) for signal processing and interfacing to control, feedback, timing and machine protection systems.

RF Frontend

The simplified block diagram of the RFFE electronics used is shown in Fig. 1. The basic principle of the BPM electronic and cavity design is based upon ref. [6].

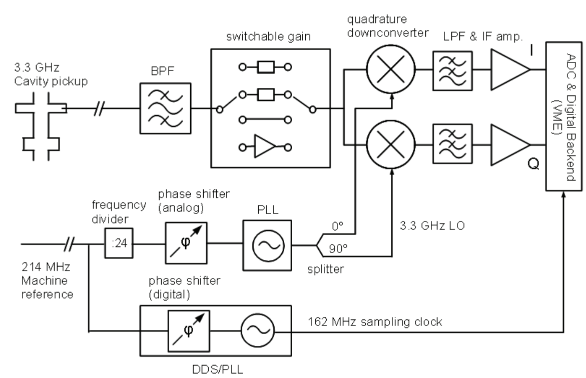

Figure 1: Simplified downconverter block diagram (one channel).

An input bandpass filter selects the cavity signal components around 3.3GHz. The filter is followed by a switchable gain section. The gain is selected depending on the actual bunch charge (4 charge ranges).

The quadrature downconverter operates with an LO frequency of approximately 3.3GHz. This frequency is equal for all three channels (reference-, x- and y-channel). A reference signal (214 MHz at the SwissFEL injector test facility, 216.66 MHz at EXFEL) is provided from the machine reference system. This signal is divided by 24 with a divider common to all LO PLLs on the RFFE.

The ADC is clocked by a signal also generated on the RFFE. Its phase is controllable in 0.5° steps around the

ISBN 978-3-95450-119-9

full circle by programming the phase tuning word of a direct digital synthesizer (DDS).
The RF front-end electronics was designed in a VME64x compliant form factor (Fig. 2).

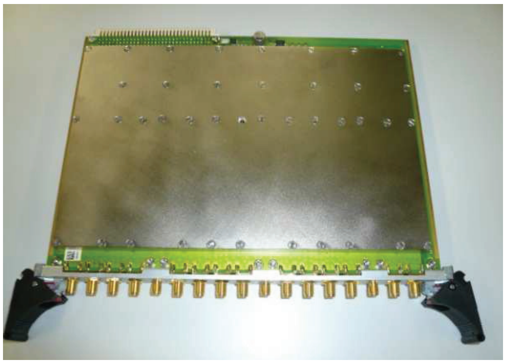

Figure 2: RF front-end card.

ADC & Digital Backend

The RFFE analog baseband signals are sampled by a 6-channel 16-bit ADC board at 160 Ms/s sampling rate. The sampling clock is provided by the RFFE. Programmable delay units allow correction of individual path delay variations for each ADC (Fig. 3).

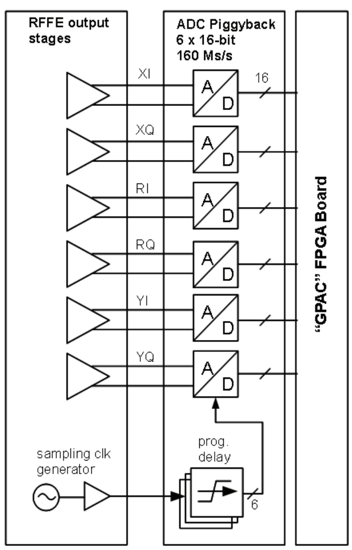

Figure 3: ADC block diagram (simplified).

The ADC mezzanine module resides on top of a VME64x compliant FPGA carrier board (GPAC = Generic PSI ADC Carrier). RFFEs and GPAC can be used both in VME64x crates, or in the so-called modular BPM unit (MBU) that will be used for the final E-XFEL BPM systems [3]. The MBU is a cost-efficient standalone crate solution with a customized backplane. The housing of the MBU provides slots for one GPAC and either two E-XFEL undulator or re-entrant cavity BPM RFFEs or four E-XFEL button BPM RFFEs, or a combination of those. By using MBU and GPAC for all BPMs in E-XFEL, a standardized interface to control, timing, interlock and feedback systems is provided. Supported protocols include Ethernet (with Linux running on the GPAC), PCIe, or custom protocols e.g. for beam based feedbacks using up to 8 multi-gigabit SFP+ transceiver links provided by the MBU.

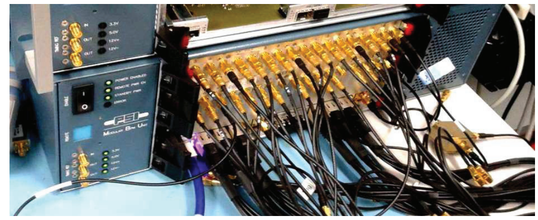

Figure 4: Lab test setup of a Modular BPM Unit (MBU), with one GPAC and two cavity BPM RFFE boards.

SIGNAL PROCESSING

RF Cavity Pulse Shape

The cavity signals as seen at the input of the RFFE electronics have a shape as seen in Fig. 5. Because of the low cavity loaded-Q factors the pulses durations is only about 20ns. High loaded-Q factor cavities providing longer pulse durations are unfavourable since bunch spacing can be as short as 222ns in the EXFEL.

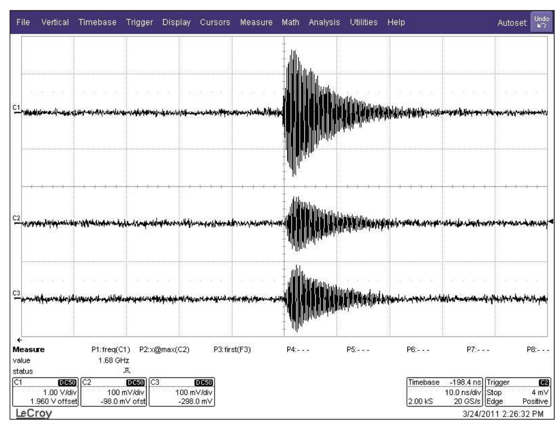

Figure 5: Cavity signals at input of RFFE (timescale: 10ns/div).

IF Pulse Shape

Down conversion and filtering in the RFFE produce baseband signals as seen in Fig. 6 top.
The IF pulses are relatively narrow compared to the sampling interval of 6.25 ns. The IF signal filter shape has been chosen to maximize S/N ratio under the condition of preventing bunch-to-bunch crosstalk. Figure 6 (top) shows an example taken from real pick up signals.
Given the short signal pulse duration the sampled vector magnitude (Fig. 6 bottom) is sensitive to the ADC sampling clock phase. Therefore, an all-digital feedback loop is used to compensate any ADC clock phase misalignment and drift (Fig. 7).

ISBN 978-3-95450-119-9

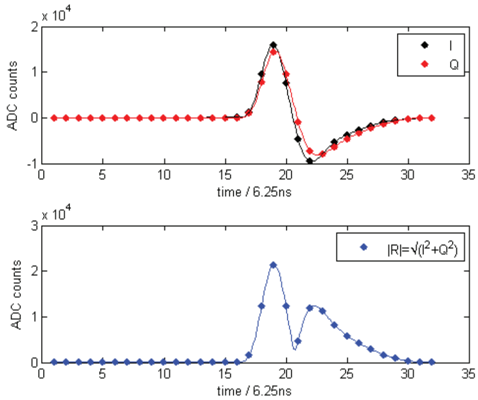

Figure 6: Baseband waveforms samples (top: I and Q signals, bottom: vector magnitude).

ADC Clock Phase Control Loop

In order to optimize signal to noise ratio and to compensate drifts occurring in beam arrival time and/or sampling clock phase the BPM electronics employs a digital phase feedback loop.

The clock phase offset is estimated from the three sampling values around the top of the reference IF vector magnitude (Fig. 6, bottom). Then the DDS clock phase is adjusted to correct this error and keep on sample at the top of the magnitude waveform (solid circles in Fig. 7).

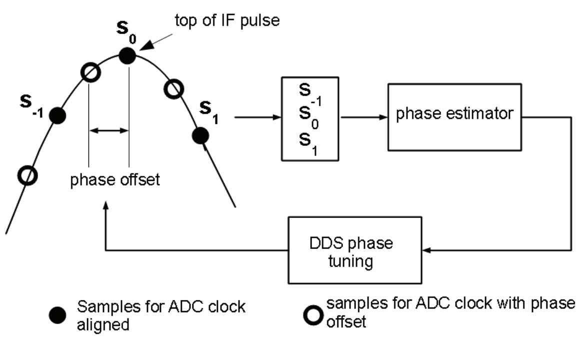

Figure 7: Principle of sampling phase alignment feedback loop.

The phase estimator currently employs a polynomial interpolation of the top section of the reference IF vector magnitude waveform. This approach allows a relatively precise estimation to be computed within a bunch spacing of 220 ns in an FPGA. Other approaches offering higher accuracy were discarded due to their higher latency.

Beam Offset Calculation

The beam offset in x direction Dx is basically calculated using the formula

$$D_X = k \cdot \frac{|X|}{|R|} \quad (1)$$

The values R and X are the peak vector magnitudes calculated from the pulse peaks of I and Q baseband waveforms of reference and x channel, respectively. For example, in Fig. 6 (bottom) the vector magnitude is represented by the value of the highest sample. k is a gain constant that we calibrate using a pickup mounted on a motorized mover with a high-resolution position encoder. In the above formula (1) $|X|$ and $|R|$ represent processed values, where downconverter I/Q imbalances and ADC offsets have already been corrected for.

TEST SETUP

In order to test the BPM system with beam an array of four BPM pickups has been installed at the SwissFEL test injector. A similar array is also installed at the FLASH accelerator facility at DESY (Hamburg). The array consists of three undulator BPM (10mm aperture) cavity pickups followed by one beam transfer line BPM (40.5mm aperture). The test results reported here were obtained using the three EXFEL undulator pickups. The test injector operates with a single-bunch repetition rate of 10Hz. Using a VME64x crate instead of an MBU allowed easy integration into the VME64x based control and timing system of the test facility. Similar measurements are planned using the cavity test array at DESY.

Figure 8: BPM test array at SwissFEL 250MeV test injector facility.

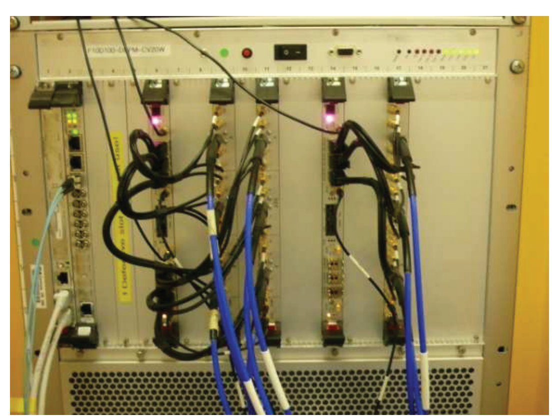

Figure 9: BPM electronics test rack (RFFE, ADC & FPGA board) at SwissFEL injector facility.

ISBN 978-3-95450-119-9

The three 10mm diameter cavities are arranged as seen in Fig. 10.

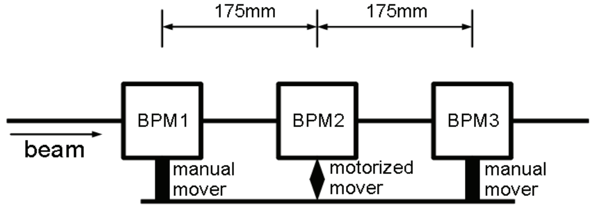

Figure 10: BPM (Ø10mm) pickup arrangement.

TEST RESULTS

Charge Resolution

Since the reference cavity TM010 mode that is coupled to the RFFE is sensitive to the beam charge only the reference channel information can be used as a sensitive charge monitor after calibration of the scaling factor by means of a dedicated charge monitor. The charge resolution R_C is determined by taking the difference of the charge readings of two BPMs and calculating

$$R_C = \frac{std(Q_1 - Q_2)}{\sqrt{2}} \quad (2)$$

std(x) is the standard deviation of the samples x.
A sample charge measurement at C≈210 pC is shown in Fig. 11. Applying (2) results in a charge resolution R_C of ≈85 fC rms.
Those values are slightly higher than the theoretical value obtained from ADC/RFFE noise calculations (Table 2).

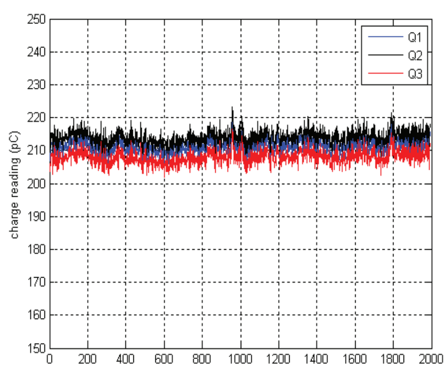

Figure 11: Charge measurement example at C≈210 pC.

Table 2: Measured and calculated charge resolutions (bunch charge ≈ 210pC)

Charge resolution at 210 pC		
Resolution Calc. From Q1-Q2	82	fC rms
Resolution Calc. From Q1-Q3	85	fC rms
Resolution Calc. From Q2-Q3	80	fC rms
Theoretical Value	70	fC rms

Position Resolution

We performed position resolution measurements based on correlating the readings of three cavities (Fig. 12). Using the position readings of BPM1 and BPM3 (d1 and d3) we calculate the difference between the linear interpolation and the displacement measured by BPM2. This difference is seen as **Δ**d in Fig. 12.

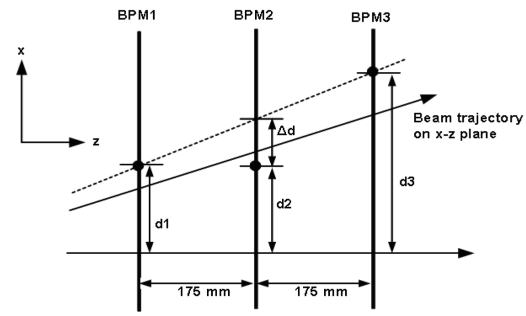

Figure 12: BPM resolution measurement using 3 cavities.

If one assumes that all BPMs have equal position jitter then the BPM resolution is

$$\delta_{BPM} = \sqrt{\frac{2}{3}} \cdot \delta_{\Delta d} \quad (3)$$

Sample data for beam position jitter measurement is seen in Fig. 13. The bunch charge during this measurement was 180pC. The RFFE gain settings were chosen to provide a linear measurement range of +/-500**μ**m.

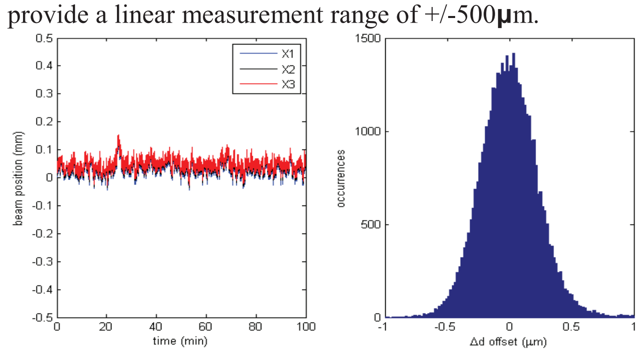

Figure 13: Sample position measurement of BPMs (180 pC bunch charge). Left: position data.
Right: Histogram of the error **Δ**d.

Calculating the distribution of the displacement **Δ**d results in the histogram seen in Fig. 13 (right). The measurement position resolution of the BPM is 183nm.
Table 3 summarizes sensitivity measurements at various beam conditions.

The rightmost column in Table 3 contains predicted values based on system noise measurement. One possible cause for the deviation from measured values is LO phase jitter that causes an increase of the position jitter of the I/Q imbalance is not fully corrected. However, the deviation could also be caused by any uncorrelated

ISBN 978-3-95450-119-9

mechanical vibrations of the three pickups (also included in the measured resolution above).

Table 3: Measured and predicted measurement jitter for different settings (x-direction)

Beam Offset (mm)	Beam Charge (pC)	Linear Meas. Range	Measured Resolution (μm-rms)	Predicted Resolution (μm-rms)
0.1	285	±2mm	0.35	0.33
0.5	285	±2mm	0.40	0.36
1	285	±2mm	0.56	0.4
0.05	183	±500μm	0.18	0.165
0.2	2	±6.4mm	11.2	13
≈0.06 varying	350	±250μm	0.12	(0.06)

It should be noted that any positively correlated noise or drift is not included in the measured resolution. Such a drift factor could be temperature drift of the electronics. Temperature drift measurements under realistic beam conditions will be conducted in near future. Measurements of the vibration levels at the pickups are also planned in order to determine the electronic resolution more precisely.

CONCLUSION

We reported first tests of the EXFEL cavity BPM electronics. The tests were performed at the SwissFEL injector facility under single-bunch conditions. First results show beam position resolution well below 1μm rms even at a linear measurement range >±1mm. These results fulfill the resolution requirements for the EXFEL undulator BPMs.

AKNOWLEDGEMENT

The authors wish to thank their colleague Daniel M. Treyer for valuable discussions and review of the RF circuit design.

REFERENCES

[1] R. Brinkmann, "*The European XFEL Project*", Proc. FEL´06, Berlin, Germany, 2006.

[2] B. Keil, et al.: "*The European XFEL Beam Position Monitor System*", Proc. IPAC, Kyoto, Japan, 2010

[3] B. Keil et al., *"A Generic BPM Electronics Platform for European XFEL, SwissFEL and SLS"*, these proceedings

[4] M. Pedrozzi, "*250 MeV Injector Facility for the SwissFEL Project*", Proc. of FEL2009, Liverpool, UK, 2009

[5] D. Lipka, et al.: "*Cavity BPM Designs, related Electronics and Measured Performances*", Proc. DIPAC'09, Basel, Switzerland, 2009.

[6] H. Maesaka, et al., *"Development of the RF Cavity BPM of XFEL/Spring-8"*, Proc. of DIPAC09, Basel, Switzerland, 2009.

[7] B. Keil, et al.: "*Design Status of the European X-FEL Transverse Intra Bunch Train Feedback*", these proceedings

ISBN 978-3-95450-119-9